Multidimensional femtosecond coherence spectroscopy for study of the carrier dynamics in photonics materials

Lap Van Dao, My Tra Thi Do, and Peter Hannaford

Centre for Atom Optics and Ultrafast Spectroscopy, School of Biophysical Sciences and Electrical Engineering, Swinburne University of Technology, Melbourne, Australia 3122
Email: dvlap@swin.edu.au

Abstract:

We present a new multidimensional spectroscopy technique based on femtosecond spectrally resolved 2-colour 3-pulse photon echoes for investigating of the carriers dynamics in the photonic materials such as semiconductor doped glass and porous silicon. The use of different colours and polarisations for the pump and probe pulses together with spectral analysis of the photon echo signals allows separation of the dynamics of electrons and holes.

Key word: *Femtosecond laser spectroscopy, multidimensional spectroscopy, photon echoes, molecular dynamics, nonlinear coherent spectroscopy*

Introduction

Following the pioneering of 'femtochemistry' by Zewail [1] in the 1980s, there has been much interest in developing *multidimensional* femtosecond laser techniques similar to those successfully used in NMR to study ultrafast dynamical processes in complex molecular systems [2-4]. These techniques include nonlinear coherent spectroscopies such as stimulated photon echoes based on sequences of femtosecond laser pulses and Raman echoes involving two or more pairs of femtosecond pulses followed by a probe pulse. Multiple-pulse nonlinear coherent techniques probe correlations between the electric fields generated in the phase-matching directions by the different pulses and allow detailed spectroscopic information to be obtained in the presence of inhomogeneous broadening. Spreading the information over more than one dimension, for example, by using several pulses with independently controllable time delays, helps to unravel and extract the complex dynamical and spectroscopic information, such as relaxation rates of the level populations, dephasing rates or homogeneous and inhomogeneous broadening of the optical transition.

We present a multidimensional spectroscopy technique based on spectrally resolved 2-colour 3-pulse photon echoes in the visible wavelength range for investigating dynamics of the excited carrier in photonic materials such as semiconductor doped glass and porous silicon.

Theoretical Background

The polarization induced in an isotropic medium by pulsed optical radiation may be expanded as a sum of terms involving odd powers of the optical electric field $\boldsymbol{E}$:

$$\boldsymbol{P} = \boldsymbol{P}^{(1)} + \boldsymbol{P}^{(3)} + \boldsymbol{P}^{(5)} + \ldots\ldots = \chi^{(1)}\boldsymbol{E} + \chi^{(3)}\boldsymbol{E}^3 + \chi^{(5)}\boldsymbol{E}^5 + \ldots\ldots, \qquad (1)$$

where $\chi^{(1)}$, $\chi^{(3)}$,…are the first-order, third-order… susceptibilities. The induced nonlinear polarization generates a signal electric field $E_S(t)$, which for low optical density and perfect phase matching is directly proportional to the nonlinear polarization. For low light intensities the nonlinear polarization is given by the third-order term $P^{(3)}$.

For excitation with three temporally separated optical pulses, having electric fields E_1, E_2, E_3 and (angular) frequencies ω_1, ω_2, ω_3, the third-order nonlinear polarization may be expressed in terms of nonlinear response theory [2]

$$P^{(3)}(t, t_{12}, t_{23}) \approx N(i/\hbar)^3 \int_0^\infty dt_3 \int_0^\infty dt_2 \int_0^\infty dt_1 \, [R_A(t_3, t_2, t_1) + R_B(t_3, t_2, t_1)] \tag{2}$$

where t_1, t_2, t_3 are time variables between pulses 1 and 2, 2 and 3, and 3 and the signal, respectively; and N is the density of states. R_A and R_B are optical response functions given by

$$\begin{aligned} R_A(t_3, t_2, t_1) = {} & [R_{II}(t_3, t_2, t_1) + R_{III}(t_3, t_2, t_1)] \times E_3(t - t_{23} - t_3) \exp[-i\omega_3(t - t_{23} - t_3)] \\ & \times E_2(t - t_3 - t_2) \exp[-i\omega_2(t - t_3 - t_2)] \times E_1^*(t + t_{12} - t_3 - t_2 - t_1) \\ & \times \exp[i\omega_1(t + t_{12} - t_3 - t_2 - t_1)] \end{aligned} \tag{3a}$$

$$\begin{aligned} R_B(t_3, t_2, t_1) = {} & [R_I(t_3, t_2, t_1) + R_{IV}(t_3, t_2, t_1)] \times E_3(t - t_{23} - t_3) \exp[-i\omega_3(t - t_{23} - t_3)] \\ & \times E_2(t - t_3 - t_2 - t_1) \exp[-i\omega_2(t - t_3 - t_2 - t_1)] \times E_1^*(t - t_{12} - t_3 - t_2) \\ & \times \exp[i\omega_1(t - t_{12} - t_3 - t_2)] \end{aligned} \tag{3b}$$

where t_{12}, t_{23} are the time delays between pulses 1 and 2, 2 and 3, respectively. R_I to R_{IV} and their complex conjugates are third-order nonlinear response functions.

When the signal is recorded with a slow detector, i.e., in a time-integrated measurement, the photon echo signal is given by

$$S(t_{12}, t_{23}) \propto \int_0^\infty |P^{(3)}(t, t_{12}, t_{23})|^2 \, dt \tag{4}$$

where $P^{(3)}$ is given by Eqs. (2), (3). In such a time-integrated measurement information about the temporal shape of the nonlinear polarization is lost and to retain such information additional measurements such as time-gated or heterodyne-detected measurements may be used [5].

An alternative way to obtain detailed information about the temporal evolution of the nonlinear polarization is to record the spectrum of the photon echo signal using a spectrometer [4]. The frequency-domain nonlinear polarization is determined by Fourier transformation of the time-domain nonlinear polarization [Eq. (2)] with respect to t:

$$\tilde{P}^{(3)}(\omega, t_{12}, t_{23}) = \int_{-\infty}^\infty P^{(3)}(t, t_{12}, t_{23}) \exp(i\omega t) \, dt \tag{5}$$

For a simple *two-level* system with transition frequency ω_{12} and (Lorentzian) *homogeneous* broadening the third order polarisation is given by

$$\begin{aligned} \tilde{P}^{(3)}(\omega, t_{12}, t_{23}) \propto {} & N\mu_{12}^4 \exp[(i\omega_3 - \gamma_1)t_{23}] \times \{\exp[-i\omega_{12}(t_{23} - t_{12})] \, \Theta(t_{12}) \, \Theta(t_{23}) \\ & + \exp[-[i\omega_{12}(t_{23} + t_{12}) + 2\gamma_{12}t_{12}]]\Theta(-t_{12}) \, \Theta(t_{23})\} \times [\gamma_{12} + (\omega - \omega_{12})]^{-1} \end{aligned} \tag{6}$$

where $\gamma_1 = 1/T_1$, $\gamma_{12} = 1/T_2$, T_1 is the population lifetime of the excited state and T_2 the dephasing time of the optical transition, Θ is the Heaviside function. For a two-level system with *inhomogeneous* broadening given by a Gaussian distribution $G(\omega) = \exp[-(\omega - \omega_{12})^2/\Gamma^2]$ (where Γ is the $1/e$ halfwidth) third order polarisation is given by

$$\widetilde{P}^{(3)}(\omega, t_{12}, t_{23}) \propto N\mu_{12}^4 \exp[(i\omega_3 - \gamma_1)t_{23}] \exp[[i(\omega_{12} - \omega) + \gamma_{12}]^2/\Gamma^2)] \times \{\exp[-i\omega_{12}(t_{23} - t_{12})] \operatorname{erfc}[i(\omega_{12} - \omega)/\Gamma + \gamma_{12}/\Gamma + t_{12}\Gamma/2] \Theta(t_{12}) \Theta(t_{23}) + \exp[-[i\omega_{12}(t_{23} + t_{12}) + 2\gamma_{12}t_{12}]] \times \operatorname{erfc}[i(\omega_{12} - \omega)\Gamma + \gamma_{12}/\Gamma - t_{12}\Gamma/2] \Theta(-t_{12}) \Theta(t_{23})\} \quad (7)$$

The inhomogeneous broadening leads to a frequency shift of $P^{(3)}(\omega, t_{12}, t_{23})$ and hence to a wavelength shift of the photon echo signal. The spectrally resolved photon echo signal intensity is then

$$S_{SRPE}(\lambda_D, t_{12}, t_{23}) \propto |E_S(\omega, t_{12}, t_{23}|^2 \propto |\widetilde{P}^{(3)}(\lambda_D, t_{12}, t_{23})|^2 \quad (8)$$

When the first and second pulses temporally overlap (or partially overlap) in the sample, the pulses interfere to create a periodic standing wave pattern, which can induce a *population grating* by absorption in the sample. In the present 2-colour 3-pulse experiments in which $\omega_1 = \omega_2 \neq \omega_3$, the probe pulse can be diffracted by the population grating in the phase-matching direction $\mathbf{k_4} = -\mathbf{k_1} + \mathbf{k_2} + \mathbf{k_3}$ with frequency $\omega_4 = \omega_3$. In this case the spectrum of the population grating signal is determined by the spectral profile of the probe pulse $I_{probe}(\lambda_D)$. The *total* nonlinear signal spectrum, including the contribution of the population grating, can then be written as

$$S_D(\lambda_D, t_{12}, t_{23}) = S_{WPE}(\lambda_D, t_{12}, t_{23}) + \eta(\lambda_D, t_{12}, t_{23}) I_{probe}(\lambda_D), \quad (9)$$

where $\eta(\lambda_D, t_{12}, t_{23})$ is the efficiency of the (transient) population grating, which is proportional to $[\exp(-t_{23}/\tau_{life}) - \exp(-t_{23}/\tau_{rise})]$, and τ_{life} and τ_{rise} are the lifetime and build-up time of the population grating, respectively.

For two-colour experiments with $\omega_1 = \omega_2 \neq \omega_3$, conservation of momentum and energy leads to the following phase-matching directions and signal frequencies: $\mathbf{k_4} = -\mathbf{k_1} + \mathbf{k_2} + \mathbf{k_3}$; $\mathbf{k_5} = -\mathbf{k_2} + \mathbf{k_3} + \mathbf{k_1}$; $\mathbf{k_6} = -\mathbf{k_3} + \mathbf{k_1} + \mathbf{k_2}$; $\omega_4 = \omega_3 + \delta\omega_4$; $\omega_5 = \omega_3 + \delta\omega_5$; $\omega_6 = -\omega_3 + 2\omega_1 + \delta\omega_6$, where the $\delta\omega$ represent frequency shifts associated with the transfer of optical coherence between transitions of different frequency. Thus, in 2-colour experiments in which $\omega_1 = \omega_2 \neq \omega_3$, the signal for $\mathbf{k_5}$ is the same as for $\mathbf{k_4}$ but with the sign of the coherence time t_{12} reversed, while the signal for $\mathbf{k_6}$ can yield additional information to that of $\mathbf{k_4}$ or $\mathbf{k_5}$.

Experiments

Our femtosecond laser system consists of a mode-locked Ti: sapphire oscillator and a regenerative amplifier which delivers 80 fs, 1mJ pulses at a wavelength of 800 nm and repetition rate 1 kHz. The laser pulses from the regenerative amplifier are split into two beams which pump two independently tunable optical parametric amplifiers (OPAs), thus providing a two-colour source of femtosecond laser pulses. Frequency resolved optical gating (FROG) measurements show that the pulses from the OPAs, when optimised, have a very little linear chirp. The OPAs have several options for frequency generation – second harmonic generation (SHG), fourth harmonic generation (FHG) or sum frequency generation (SFG) – allowing coverage of a broad range of wavelengths (250 – 2000 nm) with pulse duration of about 100 fs. The FWHM of the spectral profile of the pulses from the OPAs is 250 – 350 cm^{-1} (7 – 12 nm in visible wavelength range). The output of the first OPA is split into two beams, which act as the pump pulses $\mathbf{k_1}$ and $\mathbf{k_2}$, and the output of the second OPA acts as the probe pulse $\mathbf{k_3}$. The three pulsed beams with time delays t_{12} and t_{23} are aligned in a triangular configuration and focussed by a 15 cm focal length lens into the sample. The signal is measured in the phase-matching directions $\mathbf{k_4}$ and $\mathbf{k_6}$ and detected by

one or more spectrometers equipped with CCD array and having spectral resolution of about 1 nm.

Results and discussions

Study of semiconductor doped glass

i) Detection of $k_4 = -k_1 + k_2 + k_3$: The fig. 1 shows the spectrum of the signal in k_4 direction with a fixed delay between pulse 1 and 2 at $t_{12} = 0$ fs (fig.1a,b) and between pulse 2 and 3 at $t_{23} = 0$ fs (fig.1c,d), and scan other the delay t_{23} and t_{12} respectively. The laser wavelength is $\lambda_1 = \lambda_2 = 580$ nm and $\lambda_3 = 600$ nm. At the short delay time (-100 fs to 100 fs) the signal has a wavelength at $\lambda_4 = \lambda_3 + \delta\lambda_4$, where $\delta\lambda_4$ represents the wavelength shift that reflect the dynamics of electrons and holes associated with coherence memory during the intraband relaxation. When the polarisation of three laser beams are parallel (P-polar, Fig. 1a,c) the A and B-holes with band splitting about 20-30meV have a same contribution to observed signal the spectrum of photon echo is broader then for the case the polarisation the probe beam is perpendicular to pump beams (S-polar, Fig. 1b,d). A transient grating signal is observed for long delay by scanning of t_{23}.

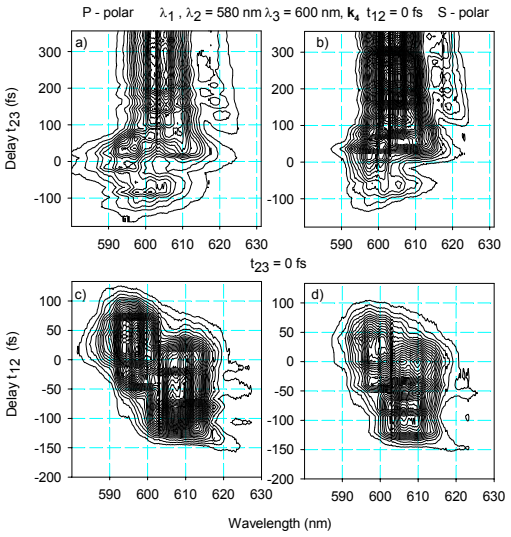

Fig 1: Time evolution of nonlinear signal spectrum detected in $\mathbf{k_4}$ direction: a,b) verus delay time t_{23} at fixed delay time $t_{12} = 0$ fs, and c,d) for verus delay time t_{12} at fixed delay time $t_{23} = 0$ fs

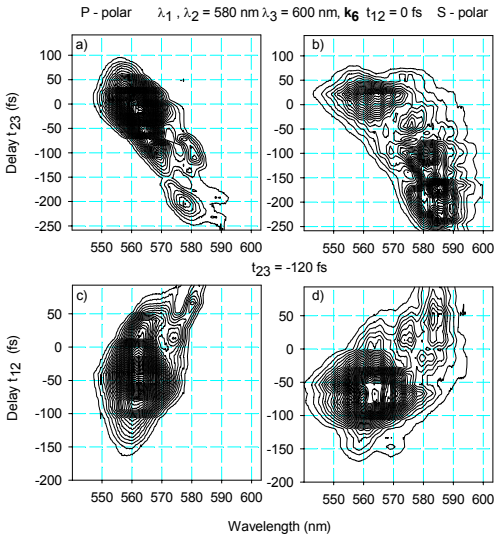

Fig 2: Time evolution of nonlinear signal spectrum detected in $\mathbf{k_6}$ direction: a,b) verus delay time t_{23} at fixed delay time $t_{12} = 0$ fs, and c,d) for verus delay time t_{12} at fixed delay time $t_{23} = -120$ fs

ii) Detection of $k_6 = -k_3 + k_1 + k_2$: For detection in the phase-matching direction $\mathbf{k_6} = -\mathbf{k_3} + \mathbf{k_2} + \mathbf{k_1}$ the photon echo signal has a wavelength $\lambda_6 \approx -\lambda_3 + 2\lambda_1 + \delta\lambda_6$. For $t_{12} = 0$ fs a "pure" four wave mixing signal at 560 nm can be observed if three pulse is overlap in time ($t_{23} = 0$ fs, fig. 2a,b). At the time delay $t_{23} = -120$ fs (fig. 2c,d) for detecting in $\mathbf{k_6}$ direction the pulse $\mathbf{k_3}$ precedes $\mathbf{k_2}$ and $\mathbf{k_1}$, and the 'coherence time' is now given by t_{23} and the 'population time' by t_{12} . The observed signal on negative delay t_{12} (fig. 2c,d) (also for $t_{23} < 0$) is the stimulated photon echo that reflect the intraband relaxation of excited electrons holes. The change of spectral width in the case of perpendicular polarisation of probe pulse involves the dynamics of excited electrons.

Study of porous silicon

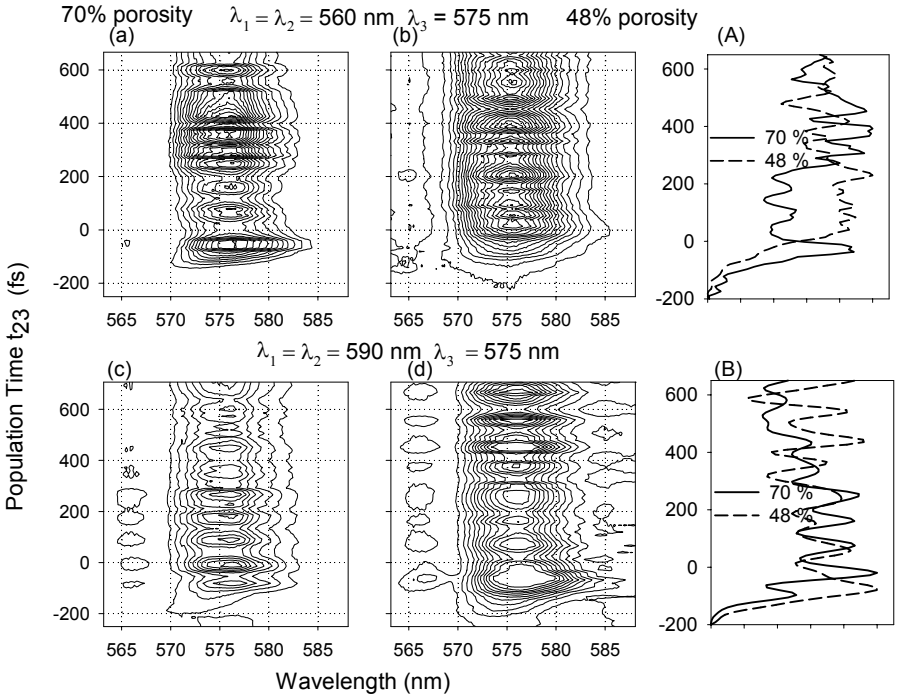

Fig 3: Spectra of the nonlinear signal in $\mathbf{k_4}$ direction verus the delay time t_{23} with fixed $t_{12} = 0$ and $\lambda_3 = 575$ nm for a) sample with 70% porosity and $\lambda_1 = \lambda_2 = 560$ nm; b) sample with 48% porosity and $\lambda_1 = \lambda_2 = 560$ nm; c) sample with 70% porosity and $\lambda_1 = \lambda_2 = 590$ nm; d) sample with 48% porosity and $\lambda_1 = \lambda_2 = 590$ nm. The insets plot the signal intensity at 750nm with spectral window of 2 nm A) for the case in fig 2a and 2b and B) for the case in fig 2c and 2d.

Fig. 3 displays the echo spectrum verus delay time t_{23} with the fixed of $t_{12} = 0$ fs in the fist 1 ps. Similar spectrum is observed for the fixed $t_{12} = \pm 40$ fs but the intensity is small. Clear oscillations can be seen in all case. When the laser pulses cover or partly cover two (or more) transitions with frequencies ω_i, ω_j, two different quantum pathways can be involved by interaction of system with laser pulses, which can interfere, and the time-integrated signal versus delay time t_{12} or t_{23} can exhibit oscillations (or quantum beats) at the difference frequency $\Delta\omega = | \omega_i - \omega_j |$. Fourier transformations of the signal intensity verus the decay time provide some splitting energy. In all case a energy splitting of 4-5 meV can be observed that close to singlet and triplet splitting (6meV [6]) of Si crystal or spin-orbit splitting of conduction band of porous silicon quantum wire (3-7 meV [7]). A splitting of 18meV and 22 meV is deduced for sample with 48% porosity and 21 meV and 28meV for sample with 70% porosity. This energy splitting is closed to the magnitude of the spin-orbit splitting of the valence band is around 20-35 meV [7]. For the case of pump wavelength at 560 nm and probe wavelength at 575 nm the rise time (the time for signal reaches its maximum) is longer (up to 500 fs) for sample with high porosity (70%) as see in Fig 2a or on the inset 2A. Similar result is obtained when the pump at 575 nm and probe at 590 nm have been applied. The rise time can be the time for localise of excited electrons in conduction band.

Conclusions

Spectrally resolved 2-colour 3-pulse photon echo spectroscopy in the visible provides a potentially powerful multidimensional technique for studying dynamics of excited carriers on a femtosecond time scale. The detection of the spectra of the photon echo signals in a spectrometer equipped with CCD detector provides a convenient way of obtaining an additional dimension without the requirement of an additional scan (and hence additional data collection times). In particular, the multidimensional spectra can be used to probe the time evolution of the amplitude of the third-order nonlinear polarization induced in the sample by the three laser pulses. The large number of available degrees of freedom allows one to separate and extract certain specific types of spectroscopic information in complex systems. The use of different colours for the pump and probe pulses together with spectral analysis of the photon echo signals allows separation of the dynamics of electrons and holes. The use of spectrally resolved photon echoes also allows the resolution of different quantum beat frequencies corresponding to different selected energy levels.

Acknowledgments

We thank Mark Aizengendler and Alex Stanco from Lastek Laboratories, Thebarton, Australia for their contributions to the multi-channel detection system with Garry CCD array. The porous silicon samples were made by Peter Reece from School of Physics of the university of New South Wales. This project is supported by a Swinburne University Strategic Initiative Grant and an Australian Research Council Discovery Grant.

Reference

1. See, e.g., A.H. Zewail, Femtochemistry – *Ultrafast Dynamics of the Chemical Bond*, Vols I, II (World Scientific, Singapore, 1994).
2. S. Mukamel, *Principles of Nonlinear Optical Spectroscopy* (Oxford University Press, New York, 1995).
3. S. Mukamel, A. Piryatinski and V. Chernyak, Acc. Chem. Res. **32**, "*Two-dimensional Raman Echoes: Femtosecond view of molecular structure and vibrational coherence*" 145-154 (1999).
4. L. V. Dao, C. Lincoln, M. Lowe and P. Hannaford *"Spectrally Resolved Femtosecond Two-Colour Three-Pulse Photon Echoes: Study of Ground and Excited State Dynamics in Molecules"*, J. Chem. Phys. **120**, 8434-8442 (2004).
5. W.P. de Boeij, M.S. Pshenichnikov and D.A. Wiersma, Chem. Phys. **233**, "*Heterodyne-detected stimulated photon echo: applications to optical dynamics in solution*", **287-309** (1998), and references therein.
6. M. Rosenbauer, S. Finkbeiner, E. Bustarret, J. Weber, M. Stutzmann, "*Resonantly excited photoluminescence spectra of porous silicon*", Phys. Rev. **B 51**, 10539-10547 (1995).
7. G. D. Sanders and Yia–Chung Chang, "*Theory of optical properties of quantum wires in porous silicon*", Phys. Rev. **B 45**, 9202–9213 (1992).